

A single loop thermoacoustic engine model performance at various ramp angle of two conical segments

Nurpatricia^{1,*}, AgusDwi Catur²

^{1,2}Mechanical Engineering Dept., Faculty of Engineering, Mataram University, INDONESIA

*Corresponding Author

ABSTRACT: Thermoacoustic engine is one of recently emerge external combustion engine that capable to utilize low grade or untreated biomass combustion as its heat source. In this article discuss the performance of a travelling-wave single-loop thermoacoustic engine model that has been built with Delta-EC simulation. The simulation conducted to study the effect of three cones with different ramp angle existence on acoustic energy losses. The results are elaborative comparison of acoustic energy losses in base engine model installed with four different segments, and four of their geometric identical counterparts that placed in reverse orientation. The segments are straight segment, cones with 30°, 45°, and 60° ramp angles. Minor losses caused by straight model is 0,46 watt in positive direction enlargement, while on average 0,23 watt caused by three cones of different ramp angle. This shows that the cones can lower the energy losses of about half. Cone with 0,88 cross sectional ratio seems less affected to different ramp angle applied. On ramp angles 30°, 45°, and 60° cones, minor losses are 0,22, 0,23, and 0,24 watt respectively.

NOMENCLATURE

Symbol	Description	Unit
A	Area	m^2
E	Acoustic energy	watt
Im	Imaginary part of complex variable	
K	Minor losses coefficient	
p	Pressure	Pa
Q	Heat	watt
Re	Real part of complex variable	
T	Temperature	K
U	Volumetric velocity	m^3/s
u	Velocity	m/s
W	Length	m
x	x-axis, x-direction	

Greek letter

ϕ	Phase angle	deg
θ	Ramp angle	deg
η	Efficiency	%

Subscripts

H	heat
A	acoustic
m	mean
1 to 6	position in x-direction

Date of Submission: 20-10-2024

Date of acceptance: 04-11-2024

I. INTRODUCTION

The ability of thermoacoustic engine to utilize untreated biomass as its heat source opens one of the promising possibilities in global climate change mitigation. The climate issue is one of the current challenges for humanity, so awareness has emerged to begin diminishing the utilization of fossil fuels which are still the main supply for global energy fulfillment, reaching 81% according to the World Bioenergy Association. The fossil fuel is considered the largest contributor in global greenhouse gas emissions, which are the main driver of climate change. The use of fossil fuels has begun to be replaced by renewable energy source, including biomass. Apart from being a household fuel, biomass can also be used in external combustion engines such as

thermoacoustic engine, Sertolli et al [1].

In order to transform biomass into high-quality fuel needed by internal combustion engines, it should be first purified. There is some equipment capable to convert biomass into a high-grade fuel state at small scale capacity, such as for household needs in rural areas. But such technology is still uncommonly available. This limitation is mainly due to the need of supporting equipment in the process which is still quite complex, and initial installation costs still relatively high. These issues restrict of biomass usage as fuel in internal combustion engines. Therefore, biomass as a fuel is more common applied in external combustion engine implementations, Elferink and Steiner [2].

A typical arrangement of a thermoacoustic engine model, which is capable in utilizing flue gas from biomass combustion as a heat source, is developed by Nurpatricia et al [3]. This model has parameters that derived from advantageous key factors of Yazaki et al [4] and Backhaust and Swift [5] engine designs. This engine model designed with special feature in hot heat exchanger arrangement which allows it to receive heat from direct flue gas flow of low-grade biomass combustion. Considering abundant availability of low-grade biomass such as agricultural waste in rural area, this type of engine arrangement has promising small scale implementation in that area.

The engine loop of this model [5] is construct as continuous passage without any bends or cross-sectional area change. As the consequences, the working fluid inside the loop is flowing without experiencing any type of losses. This idealization behavior is unrealistic compared to the fact that the actual flow undergoes energy loss due to surface friction or pressure drop. Nurpatricia and Catur [6] further develop that previous model [5] with additional of minor losses sub model of two conical segments. In this article can be found simulation result presenting performance of further modifications on that existing two cone segments. Both of conical segments are altered on their ramp angle to simulate the effect of different flow pattern that occurs inside those tapered segments.

II. SIMULATION SETUP

A. Engine Modelling

Figure 1 shows the single loop thermoacoustic engine model presented in this article. The engine model built and examined through simulation in open source software Delta EC Version 6.2, Ward et al [7]. The body of that engine is divides into several individual parts, that is regenerator (REG), hot heat exchanger (HHX), loop passage (DUCT), and cold heat exchanger (CHX). The simulation conducted regards to a cross-sectional area datum correlated to $x = 0$ position, which is marked as point 2 in Figure 1a. Acoustic energy is generated in the regenerator, or segment 3-4, of the engine. The loop starts from point 5 to point 2, which is kept in constant length at all simulation cases in this article. Acoustic energy E that flows along the loop, varies depending on its given location. Flow losses occurred in sudden change hydraulic diameter, such as sudden enlargement from point 1c to 2, will inherently take account by software through simulation process. The same condition is also applicable in the sudden contraction in segment from point 5 to 6c.

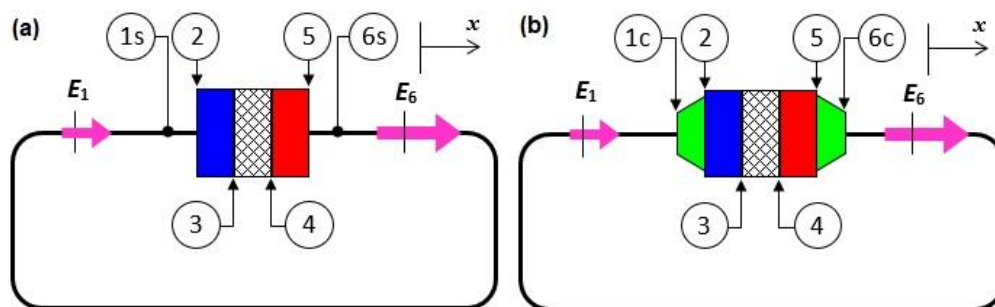


Fig. 1 The single looped thermoacoustic engine model at the interface between segments having different cross-sectional hydraulic diameter, with (a) sudden contraction interface, (b) cone segments inserted

Heat input source for this engines HHX is modeled came from hot flue gas of external low-grade biomass combustion. The heat is required to create a working fluid temperature gradient between two ends of the regenerator cross sections, that is from point 3 to 4. The working fluid temperature gradient along the regenerator is made possible by the difference in the amount of heat supply in CHX and HHX. The CHX segment is located at cross-section 2-3, and the HHX is at 4-5. Acoustic energy amplified by REG (E_4) at 4 is the location where acoustic energy is at its highest level possible. Then acoustic energy travels across HHX and it attenuated as it proceeds further along positive x direction until crossing CHX and reaching point 3 to become at

level of E_3 . The E_3 state is the lowest acoustic energy level in the entire engine location. In the case of engine model in Fig. 1a, if the cross-sectional area of loop A_{1s} or A_{6s} are the same as the cross-sectional areas of CHX and HHX, that are A_2 and A_5 , then there will be no minor losses experienced by fluid flow at these two locations.

Amount of acoustic energy E level at a given location at x throughout all segments and loops induced by two acoustic wave components, (a) traveling wave pressure wave p , and (b) the volumetric flow rate U . The variables of E , p and U are in complex domain. Therefore, relative differences in p and U oscillations leads to a specific phase difference. So that the phase difference also has an effect on the acoustic energy at both two cone segments existing in the engine's loop. The acoustic energy flowing through a certain segment in the engine model is according to the equation from Swift [8]. The acoustic energy flowing in a straight channel segment, for example between points 1s and 2 in Fig.1a, is calculated based on the pressure difference between both endpoints of the segments. This approach applies to all segments, except for the regenerator which contains the ability to convert heat into acoustics. Acoustic energy generated from regenerator segment can be calculated with Eq.1 [8]. Statement in this equation is in the complex domain, so that the pressure oscillation p and the volume flow rate U are also in the complex domain. Moreover, acoustic propagation is then represented by the statement of real component, $Re[]$ in terms on the left side and imaginary component $Im[]$ in the second right side of it.

$$\frac{1}{2} Re[gpU] = \frac{1}{2} \frac{1}{Tm} \frac{dTm}{dx} Re[pU] Re[f_k] + \frac{1}{2} \frac{1}{Tm} \frac{dTm}{dx} Im[pU] Im[-f_k] \quad (1)$$

Temperature gradient (dTm/dx) in Eq.1 is gained as an effect of heat input amount difference between heat input rate Q_{cat} at CHX and heat input rate Q_H at HHX. If the CHX is maintain at the ambient temperature, or at the engine's mean temperature Tm , the heat input of the engine is simply affected by heat injected into the HHX Q_H . Thus, the overall engine efficiency is known from Eq.2 [4,8]. Acoustic energy always attenuated along positive x direction. The only location acoustic energy is generated is inside regenerator, at its porous filling material. So that the overall efficiency is simply the ratio between acoustic energy amplification by regenerator E and heat input Q_H injected into HHX.

$$\eta_{H-A} = (E/Q_H) \quad (2)$$

$$E = \frac{1}{2} |p| |U| \cos(\phi_{pU}) \quad (3)$$

The acoustic energy in every location of the engine including conical segments if exist, except regenerator, is following Eq.3 [7,8]. Not only pressure p and volumetric velocity U waves are dominant factors in determining acoustic energy, but also phase angle difference ϕ between both of them.

B. Minor Losses

The engine model of Nurpatra et al [3], as shown in Fig.1a, is built with some geometrical simplifications, including that the loop channel composed without bends, diameter alteration, or conical segments. Such idealization assumption lead to impracticality in the manufacturing process. The real engine loop channel usually assembled from several single piece of pipes and bends that connected together to form a complete single loop. As a consequence, the engine model must be refined to accommodate those various different type of physical geometries form that may exist in the loop channel.

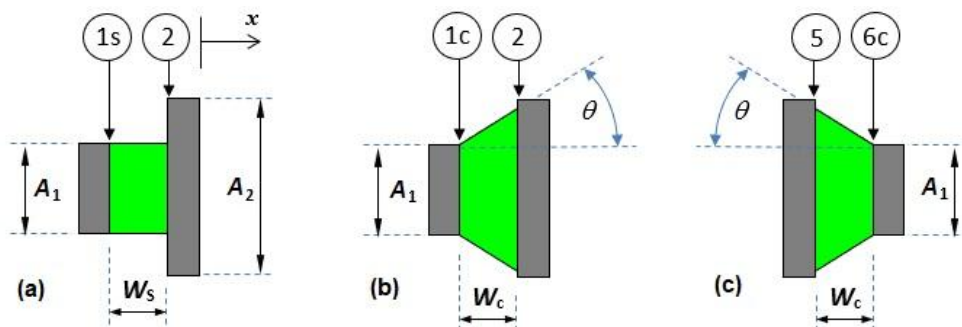


Fig. 2 A sudden enlargement interface (a) is replaced by a corresponding conical segment (b). A sudden contraction interface, which is in opposite direction of (a) is also replaced by conical segment (c), and each of those cones has a certain ramp angle θ .

That more realistic channel model in turn leads to further modelling improvement on flow losses that occurred at those geometries. Flow losses, or commonly termed as minor losses, such as bend segment and diameter changes are added in the model of Nurpatra and Catur [6]. Two segments of cone-shaped are introduced into the model in order to compensate the effect of minor losses, Fig.1b. The first segment is placed before CHX at 1c-2, detail in Fig.2b, and the second segment is located after HHX at 5-6c, as shown in Fig.2c. Both of the segments are identical, but vice versa in orientation toward x direction.

Minor losses (Δp) in the loop of a thermoacoustic engine is adapted from Ward et al [7]. It depends on coefficient K, and the flow velocity u, in Eq.4. The velocity u is volumetric flow rate in the complex expression U from Eq.1, and it is reciprocal along x direction. So that the numeric value of K factor in Eq.4 should be set individually for each positive x-direction flow (K+) or negative x-direction flow (K-). Pressure p in x direction will decrease due to inner friction of working fluid particles flowing through inner wall surface roughness, and it indicates by minus sign in Eq.4. In conducting the simulation, both K+ and K- is set simultaneously inside the software through sub model for each conical segment, Nurpatra and Catur[6].

$$\Delta p = -\frac{1}{2}Ku^2 \tag{4}$$

This paper presenting performance of the engine model at three different ramp angles, that are 30°, 45°, and 60°, so that the effect of them in each cone segment that causing minor losses can be revealed. In comparison, the engine's performance at correlated area sudden contraction of straight segment, or at 90° transition, is also investigated. All that four cases are investigated in identical HHX, CHX, and REG setup parameters. Heat input supplied into HHX for all simulation cases in this paper is the same, 815 watts. In addition, the length of the engine's model main loop, from cross-section 5 to 2 in Fig.2a or 2b, for those four cases is maintained at constant length at 1740 mm. This current model loop length is equal to the length of previous model [6].

Table(1). Straight and cone segment ramp angles setting [9,10]

Segment		Straight		Cones					
		0		30		45		60	
Ramp Angle θ (deg)		0		30		45		60	
Location in Fig.1		1s - 2	5 - 6s	1c - 2	5 - 6c	1c - 2	5 - 6c	1c - 2	5 - 6c
1	K+	0.10	0.80	0.10	0.02	0.10	0.04	0.10	0.07
2	K-	0.80	0.10	0.02	0.10	0.04	0.10	0.07	0.10

Table 1 shows parameter of both cone segments in thermoacoustic engine on this paper [9,10]. The engine loop length of current engine model presented in this paper is also kept at the same loop length. Cone 1 length W_{c1} replaces the same length from 1 to 2 at the straight model. Also, cone 2 length W_{c2} replaces straight length W_{s2} from 5 to 6. A straight segment, Fig.2a, is replaced by a cone segment in Fig.2b. The first cone segment inserted into the model is placed at cross section 1 to 2, and the second one is at 5 to 6 (not shown in figure 2) but in reverse convergent direction, Fig.2c. The cone diameter, or hydraulic diameter, of the first cone is gradually enlarges from its smallest inner diameter D_1 at 1, derived from cross-section A_1 at the same location, to become largest inner diameter D_2 from A_2 at 2. So that the minor losses coefficient applied to the model in Figure 1 become K+ sets at location 1, and K- sets at location 2. In the case of the second cone, K+ sets at 5, and K- sets at 6, Fig.1 [7,9]. This two K value correlated to two different type of obstruction minor losses, gradual cross section enlargement losses in the first cone, and gradual cross section contraction losses in the second cone. In this article, A_1 and A_6 are the same at 0,009 m², and A_2 and A_5 are also equal to 0,010 m².

III. RESULTS AND DISCUSSION

The current engine model is modified from the previous model of Nurpatra and Catur [6]. This paper presented some insight of its performance when inserted separately with various shape of cone segment ramp angle, to mimic the real operational conditions of cone that commercially available in the market. The current engine model simulation shows an evolution of acoustic energy (E) level along its loop, which has similar trend compared to previous one [6], is shown in Fig.3. In the case of straight segment, acoustic energy level varies as position proceed along x positive. Point x = 0 is set before CHX at point 1s in Fig.1a or 1c in Fig.1b. Trend of energy level in straight segment also appears similarly with the result shown by all three cases of ramp angle. Fig.3 is the result of simulation conducted on Delta EC software. It shows a typical curve of acoustic energy level of the engine model inserted with two identical cones, at location 1-2 and 5-6, with ramp angle of 45°. Similar trend also happen when cone with ramp of 30° and 60° are inserted into engine's model.

Acoustic energy that passes through inlet side of CHX is 163 watts, at location $x = 0,12$ m as shown in Fig.3. The level of acoustic energy at the same location in all those different cone shapes is also varies slightly due to different minor losses experienced by each of them. Acoustic energy exits CHX then enters regenerator segment. The regenerator then increases the acoustic energy level according to Eq.1, as indicated from point 3 to point 4 in Fig.3. The main source of the acoustic energy is from heat energy of HHX, that acts as hot side temperature T_h . The temperature gradient then maintained between T_h and T_c . Figure 3 shows the highest acoustic energy generated by the engine is at point 4, that is $E_4 = 203.9$ watt. Acoustic energy along the loop then further attenuated, as shown by constant curve declination from HHX hot exit at point 5 to cold inlet of CHX at point 2. Significant acoustic energy loss induced by CHX and HHX, that is at point 2 to 3 in CHX, and at point 4 to 5 in HHX. This energy attenuation at entire loop and segments mainly due to working fluid flow frictional loss in the inner wall surface of the channel [9].

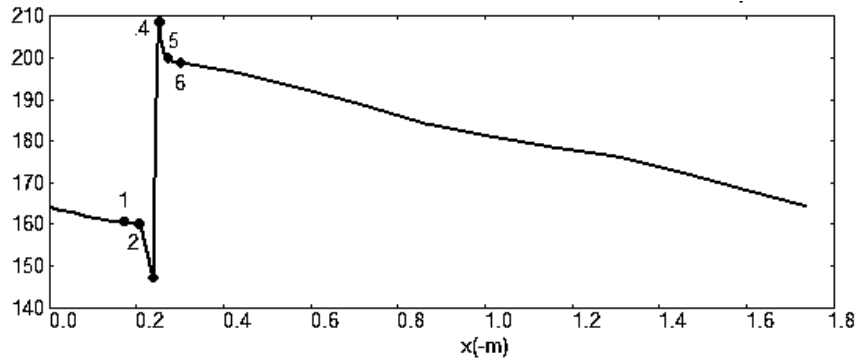


Fig. 3 Acoustic energy (E) level along the engine’s loop

Typical pressure (p) and volume velocity (U) along the engine’s loop is shown in Fig.4. The acoustic energy generation in regenerator, marked as point 3 to 4 in Fig.3, correlated to the steep pressure drop shown in Fig.4. The pressure and velocity energy are converted into acoustic energy according Eq.1. The position of regenerator is intentionally set through simulation in a certain location where the pressure is in its highest magnitude, that is at $x = 0,22$ m, and the velocity in the range of lower rate. The placement of the regenerator in the highest pressure based on consideration that the location is the highest energy level available that can be converted into acoustic energy. In contrary, the engine parameter should be adjusted so that the regenerator is at a certain location of the lowest possible velocity. Avoiding high volume velocity pass through dense porous material inside regenerator is intended to reduce working fluid friction loss.

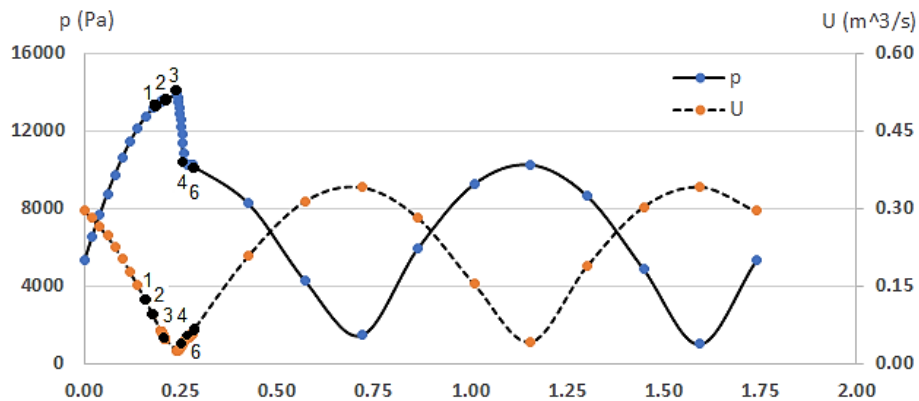


Fig. 4 Pressure (p) and volumetric velocity (U) inside the engine

Maximum pressure reached is 13,67 kPa at $x = 0,2093$ m at point 3 in Fig.3 and Fig.4, that is at inlet side of the regenerator. At that pressure the volume velocity is $0,05$ m^3/s and their magnitude have phase angle ϕ of -47.40 degree. Inside regenerator pressure drops about 3,30 kPa, and the phase angle shifted into -56.11 degree. The p and U wave oscillating in $2T$, two period mode. Pressure drop from point 3 to point 4 in Fig.4, depicts the heat to acoustic energy conversion process as shown in Fig.3, step increase of acoustic energy from point 3 to 4. As a result, the overall heat to acoustic conversion process according to Eq.2 of this model with 45° cone ramp undergoes at efficiency of 6,93%. Heat to acoustic engine model efficiency with straight segment, 30° and 60° cone ramp, are 6,90%, 6,93% and 6,92% respectively.

Result of simulation conducted in four different setting of engine model in Fig.5 shows the acoustic energy losses experienced by each cone. Minor losses occurred in all segments 5-6 is generally higher than those in segments 1-2. In the case of straight segments, the losses in segment 5-6 is around twice as much of in segment 1-2. The losses at all cones in segment 5-6 even higher, they are exceeding 3 times compared to losses at all cone segments 1-2. Interesting to note that two identical segments, applied in both straight and cone segment, could induced significantly different acoustic minor losses level. For instance, in 45° ramp angle cone the minor losses at cone segment 1-2 is 0,21 watt but in segment 5-6 the loss more severe up to 0,82 watt. This tends to happen in all four cases.

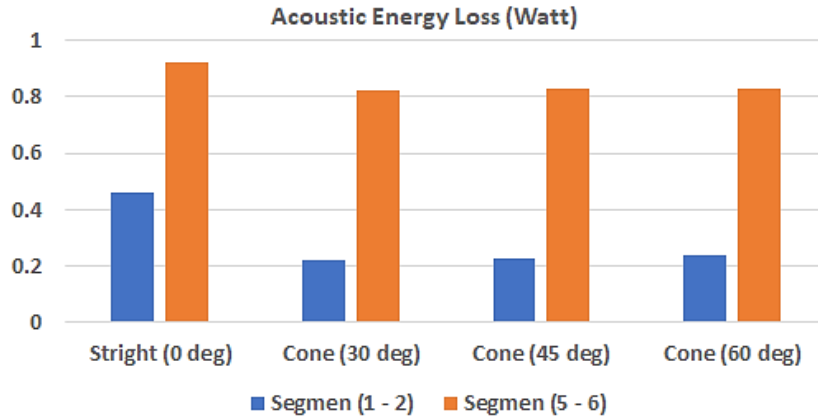


Fig. 5 Acoustic energy (E) minor loss at different segment

Several factors are predicted to have an influence so that the simulation result depicts this phenomenon on Fig.5. Detail study and numerical simulation in Gonzales et al [11] shows that relatively violent and abrupt fluctuation in flow more intense in sudden cross-section change, such as in straight segment in Fig.5. The intensity of abruptness becomes lower if that straight segments are replaced by cone segments. It is apparently observed in the segments at section 1-2, that the acoustic energy loss of a straight segment is twice as high compared to energy losses in all cone segments. Simulation results of the above-mentioned in Gonzales et al [11], are also in line with Popov et al [12]. Another factor is the relative position of each segment along the engine's loop. Since acoustic energy depends on three variables according to Eq.3, pressure and velocity magnitudes are different at a certain location in the x-direction, as well as the phase angle between the two as shown in Fig.6. Phase angle ϕ at location 1-2 is relatively the same in four segments, that is -60° with a variation under 1%. In contrast, ϕ of four segments in 5-6 is about 42° also with under 1% variation.

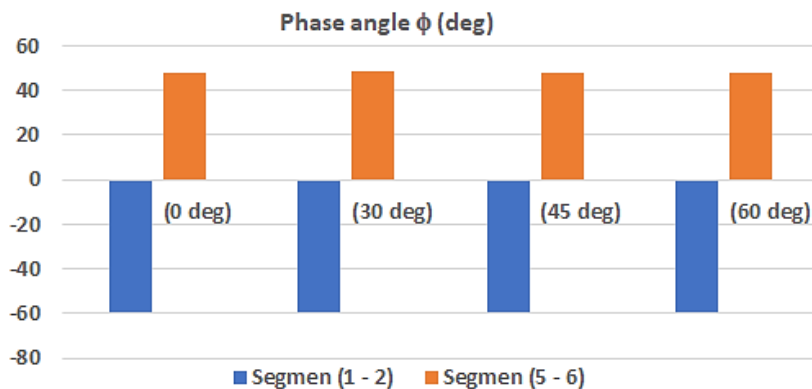


Fig. 6 Phase angle ϕ between pressure (p) and volumetric velocity (U)

The highest acoustic energy loss in all simulation results is 0,92 watt at a straight segment 1-2, while the lowest is 0,22 watt at a ramp angle of 30° of a cone segment 1-2. At the same type of segment, namely straight and cone with three ramp angles, acoustic energy loss of a segment in positive x-direction orientation tends to better mitigate minor losses. Compared to heat input at HHX of 519 watts, even the highest acoustic energy losses are only a tiny fraction. This is due to the high ratio diameter (D_1/D_2) of 0,9. At lower values of (D_1/D_2) in Fig 2a, 2b, and 2c, fluid flow tends to experience a greater acoustic loss [11]. According to Fig.5, the replacement of a straight segment with cones is relatively effective in reducing energy losses.

IV. CONCLUSION

This paper presents the results of simulation conducted to study the insertion effect of three cones with different ramp angle on acoustic energy losses. The results are compared to losses that obtained in the base engine model with straight model of sudden change cross-sectional passage interface. Other comparative result is observed between two identical segments that is placed in vice versa orientation. Acoustic energy minor losses induced by cones is half lower on average than those compare to losses from straight segment. Relative position and orientation of cone is an affecting factor as well. In two identical straight segments, the losses difference up to double in gap. Meanwhile, the losses level gap of two identical cone at the same ramp angle with different orientation is three times.

REFERENCES

- [1]. Sertolli A., Gabnai Z., Lengyel P., Bai A. [2022] "Biomass potential and utilization in worldwide research trends - A bibliometric analysis" *Sustainability*, Vol. 14, No. 5515
- [2]. Elferink M, Steiner T. [2019] "Thermoacoustic waste heat recovery engine - Comparison of simulation and experiment" *Proceedings of Meetings on Acoustics*, Vol. 35, No. 065002
- [3]. Nurpatria, Susana I G.B., Joniarta I W., Nurchayati, Tira H.S. [2021] "Peningkatan efisiensi konversi energi mesin termoakustik" *Prosiding SAINTEK LPPM Universitas Mataram*, Vol. 3, pp.369-373
- [4]. Yazaki T., Iwata A., Maekawa T., Tominaga A. [1998] "Traveling wave thermoacoustic engine in a looped tube" *Physical Review Letters*, Vol. 81, No. 15
- [5]. Backhaus S., Swift G.W. [2000] "A thermoacoustic Stirling heat engine - Detailed study" *Journal Acoustic Society of America*, Vol. 107, No. 6
- [6]. Nurpatria, Catur A. D. [2023] "Minor Losses Of Cone Segments Insertion Into Single Loop Thermoacoustic Engine Model" *IJPSAT*, Vol.39 No.1, pp.177-183
- [7]. Ward B., Clark J., Swift G. [2008] *Design Environment for Low-amplitude Thermoacoustic Energy Conversion (Delta EC) - Version 6.2 Users Guide*, Los Alamos National Laboratory
- [8]. Swift G [2001] *Thermoacoustics - A unifying perspective for some engines and refrigerators*, Condensed Matter and Thermal Physics Group - Los Alamos National Laboratory, 5th Draft
- [9]. Yiyi M., Xiujuan X., Shaoqi Y., Qing L. [2015] "Study on minor losses around the thermoacoustic parallel stack in the oscillatory flow conditions" *Physics Procedia*, No. 67, pp.485-490
- [10]. Cengel Y.A., Cimbala J.M. [2014] *Fluid mechanics fundamentals and applications*, 3rd Edition, The McGraw-Hill Companies
- [11]. Gonzales J., Fernandez A.M., Perez I.V., Oro J.M.F. [2024] "Minor loss coefficient for abrupt section changes in a cylindrical pipe using a numerical approach" *Fluids*, No. 9/152, pp.1-19
- [12]. Popov G., Klimentov K., Kostov B., Dimitrova R. [2020] "Determining the minor loss coefficient of cone diffusers" *E3S Conferences* 207/04004, pp.1-10